

Bionanomaterials from plant viruses

Alaa A. A. Aljabali and David J. Evans

Corresponding author: Professor David J. Evans

Professor David J. Evans

Department of Chemistry

University of Hull

Cottingham Road

Hull

HU6 7RX

United Kingdom

E-mail:[david.evans@hull.ac.uk](mailto:david.evans@hull.ac.uk)

Dr Alaa A. A. Aljabali

Radcliffe Department of Medicine

University of Oxford

Level 6 West Wing

John Radcliffe Hospital, Headley Way, Headington,

Oxford, OX3 9DU

United Kingdom.

## **1 Abstract**

Plant virus capsids have emerged as useful biotemplates for material synthesis. All plant virus capsids are assembled with high-precision, three-dimensional structures providing nanoscale architectures that are highly monodisperse, can be produced in large quantities and that cannot replicate in mammalian cells (so are safe). Such exceptional characteristics make plant viruses strong candidates for application as biotemplates for novel and new material synthesis.

## **2 Introduction**

Bionanoscience, a sub-section of nanoscience, involves the exploitation of biomaterials, devices or methodologies on the nanoscale. It is multidisciplinary as it sits at the interface of chemistry, biology, physics, medicine, engineering and materials science. It is the combination of biology and nanotechnology that takes advantage of natural nanoparticles to create materials and devices on the nanoscale. Nanosystems may be produced by either micro-fabrication, making big structures smaller and/or by embedding smaller features into macroscopic materials (top-down), or by using the techniques of component assembly and/or supramolecular chemistry to make small molecules bigger (bottom-up). Biomaterials such as DNA, RNA, proteins, and viruses can be used as building templates for nanomaterials. Viruses in particular are of great interest to the nanotechnology field because of their highly monodisperse structures, small size, and the ability to self-assemble with high precision.

### **2.1 Viruses**

The word virus is Latin and means poison. Viruses are obligate intracellular parasites, which only replicate within a host cell. Particles of simple (non-enveloped) virus typically consist of two components: one or more capsid proteins (shells) that assemble into precise three-dimensional structures and genetic material. The genetic material is located in the interior of the capsid as circular, single-stranded or double-stranded fragments. Enveloped viruses possess a bi-lipid layer on the exterior that provides targeting specificity to the virus. Plant

and bacteria viruses (bacteriophages or phages) are not pathogenic to animals, so they are safe for use in materials science. The genome encodes the proteins necessary for the replication of the virus and the capsid protein(s); the capsid is mainly for the protection of the genetic material. Virus capsids also have roles in host cell targeting and cell entry [1]. Virus particles typically represent very stable structures that have evolved to withstand a broad range of environments yet are sensitive enough to release their nucleic acid when they infect a susceptible cell [2].

## 2.2 Why virus nanoparticles (VNPs)

Viruses are considered as protein cages, scaffolds and templates for the production of novel nanostructured materials on/in which organic and inorganic moieties can be incorporated in a very precise and controlled fashion. Genetic engineering (chimaeric technology) enables the insertion or replacement of selected amino acids on virus capsids for uses from bioconjugation to mineralization [3, 4]. Many virus coat proteins will assemble *in vitro*, naturally or after genetic manipulation, into non-infectious containers called virus-like particles (VLPs). Viruses can be found in a variety of distinct shapes, most commonly icosahedrons (sphere-like) and rod-shaped, Figure 1, though, especially in the case of bacteriophages, more complicated structures can be formed.

### *Figure 1*

Plant viruses are non-infectious towards other organisms and they do not present a biological hazard. The production of the virus particles is simple and quick. When produced in the natural host, high expression yields can be achieved. For example, some plant virus particles can be obtained in gram scales from 1 kg of infected leaf material within 2–4 weeks [5]. Heterologous expression systems can also give rise to high yields of VLPs [6]. Viruses have unique properties: ease of functionalisation, ability to self-assemble, monodispersity, structural symmetry and the majority of viruses are stable over a wide range of pH and

temperatures. Further, they display a remarkable plasticity in their capsid structure and dynamics (coordinated assembly, disassembly and uniformity). Their amenability to genetic and chemical modification and diversity of sizes and shapes make them ideal work-horses with a variety of possible applications in nanotechnology.

Many plant viruses, due to these properties, have been investigated for their potential use for material fabrication on the nano/microscale, including the icosahedral, sphere-like, viruses Cowpea chlorotic mottle virus (CCMV), Cowpea mosaic virus (CPMV), Brome mosaic virus (BMV), Cucumber mosaic virus (CMV), Red clover necrotic mosaic virus (RCNMV), Carnation mottle virus (CarMV) and Turnip yellow mosaic virus (TYMV), and the rod-shaped Tobacco mosaic virus (TMV). Viruses offer three different surfaces that can be exploited: the exterior, the interior, and the interface between subunits, Figure 2. The inner cavity of the virus capsid is accessible to small molecules and impermeable to larger ones, which allows the use of the interior space of VLPs as nanotemplates and nanoreactors. Furthermore, the exterior surface is widely considered as a robust platform and is used for both chemical and genetic modification allowing multivalent ligand display. The virus architectural interface is crucial for assembly and offers another route for the manipulation of the capsid architecture.

### *Figure 2*

### **2.3 Empty virus-like particles (VLPs)**

Virus-like particles (VLPs) are supramolecular structures that have the form of rods or icosahedrons with diameters in the range of 25–100 nm [7]. They are composed of multiple copies of one or more recombinantly expressed virus structural proteins that spontaneously assemble into particles upon expression. In addition to being virus-like in structure, they are often antigenically indistinguishable from the virus from which they were derived. VLPs

resemble viruses but are non-infections because they do not contain any virus genetic material.

*In vitro* assembly and re-assembly methods have been exploited for VLPs. Generally, particles are exposed to a disassembly buffer followed by dialysis against an assembly buffer. These disassembly approaches allow the release of nucleic acid and are used to generate VLPs for encapsulating materials of interest on reassembly. VLPs of TMV and CCMV have been demonstrated to efficiently self-assemble *in vitro* [8]. Alternatively, an alkaline hydrolysis method was developed to extract nucleic acid from CPMV [9] to generate empty particles. Recently, a method for the production of large quantities of CPMV VLPs in plants has been developed [10]. The mature large (L) and small (S) proteins of the capsid structure are produced by the cleavage of the precursor (VP60) by the action of a virus-encoded proteinase (24K proteinase). CPMV VLP production takes advantage of the highly efficient plant transient expression system, pEAQ-HT [11, 12]. The pEAQ-HT system is used to simultaneously express the VP60 coat protein precursor and the 24K proteinase in plants *via* agroinfiltration. Efficient processing of VP60 to the L and S proteins occurs, leading to the formation of VLPs [10, 13]. CPMV VLPs possess the same structure as wild-type CPMV but lack the genetic material within the capsid, Figure 3.

### ***Figure 3***

Virus platforms including CCMV [14], TMV [15], MS2 bacteriophage [16] and polyoma virus-like particles (capsoids) [17] have been used as constrained reaction vessels for packaging and nucleation sites for mineralization [14, 18]. In addition, intact enzymes have been encapsulated within the CCMV capsid [19]. Further examples of the use of VLPs for the production on bionanomaterials will be presented later.

For RCNMV, the decoration of preformed synthetic nanoparticles with an origin of assembly site (OAS) that initiates coat protein monomer binding leads to self-assembled VLPs with synthetic nanoparticles within. Thiolated artificial OAS was attached to gold nanoparticles and the OAS-gold nanoparticles were mixed with RCNMV coat protein monomers. This templates the *in vitro* self-assembly of VLPs around the gold nanoparticle, Figure 4 [20]. This approach was expanded to include encapsulation of quantum dots with sizes of 5, 10, and 15 nm [20, 21].

#### **Figure 4**

Alternatively, a nanoparticle is coated with negatively charged polymers to mimic RNA, an approach which was pioneered by Dragnea's group. Although citrate-stabilised gold nanoparticles resulted in VLPs encapsulating preformed gold nanoparticles the process was not efficient [22]. However, covalent functionalisation of nanoparticles with carboxyl-terminated polyethylene glycol (PEG) [23, 24] was used to mimic RNA nucleation and promote efficient *in vitro* self-assembly, Figure 5.

#### **Figure 5**

### **3 Tobacco mosaic virus (TMV)**

TMV is a rod-like plant virus consisting of 2130 asymmetric subunits arranged helically around a single-stranded RNA genome. Native TMV is 300 nm in length and 18 nm in diameter with a 4 nm cylindrical central cavity [25, 26], which can be purified from infected tobacco plants in large quantities. The surface properties of TMV have been chemically and genetically manipulated without affecting the virus integrity or morphology of the capsid. The highly polar outer and inner surfaces of TMV contain hydroxyl and deprotonated carboxylate groups [27]. TMV has been exploited as a template to grow metal or metal oxide

nanoparticles such as iron oxides, iron oxyhydroxides, cadmium sulfide, lead sulfide, gold, nickel, cobalt, silver, copper, CoPt, FePt, and silica. [28-32].

In order to achieve successful coating based on electrostatic interactions, the deposition conditions should be varied in order to match the interaction between the virion surface and the deposition precursor. In the case of silica coating, carrying out the reaction at a pH less than three results in a positively charged TMV surface that will have strong interactions with the anionic silicate sols formed by hydrolysis of tetraethoxysilane. In contrast, cadmium sulfide, lead sulfide and iron oxides can be successfully coated on the outer surface at near neutral pH by specific metal ion binding with glutamate and aspartate residues [33]. As for metal deposition, in some cases, a suitable activation agent is needed in order to realise successful coating; Pd(II) and Pt(II) are two typical activation agents. The metal deposition can occur either inside the inner channel or at the outer surface of TMV [34].

Genetically engineered TMV can show enhanced deposition of metal onto its surface [35, 36]. Native TMV can be genetically altered to display multiple metal binding sites through the insertion of two cysteine residues within the amino-terminus of the virus coat protein. *In situ* chemical reductions successfully deposited silver, gold, and palladium clusters onto the genetically modified TMV without any activation agent [35]. Furthermore, mixing TMV with aniline and a mild oxidant resulted in highly uniform, micron length nanofibres measuring approximately 2 nm in diameter, likely due to the non-covalent interactions between aniline and TMV [36].

The exterior and interior of TMV have been utilised for inorganic material synthesis via metal electroless deposition (ELD). The interior surface of TMV is negatively charged under physiological conditions, whereas the exterior surface exhibits positive charge [37]. The exterior of TMV was coated with cadmium sulfide, lead sulfide, amorphous iron oxide, silica [15], platinum and gold [38, 39]. Silver and copper can be incorporated inside the central

channel of TMV; the differential nucleation being electrostatically driven as a consequence of the difference in surface charges [40, 41]. In addition, TMV particles were engineered to encode unique cysteine residues (TMV1cys); this allowed the assembly of TMV1cys onto a gold patterned surface, the particles assembled in a vertically oriented fashion. The subsequent ELD resulted in uniform metal coatings up to 40 nm thick [42].

#### **4 Cowpea chlorotic mottle virus (CCMV)**

CCMV is a member of the bromovirus group of the Bromoviridae family. The genome consists of three single-stranded, positive sense RNAs that are encapsidated separately. The capsid is composed of 180 asymmetric (identical) protein subunits (20.3 kDa each). CCMV particles are ~28 nm in diameter formed as an icosahedral shell. Virus can be obtained in high yields of 1-2 g of purified particles per 1 kg of infected plant tissue. In addition, yeast-based expression systems of the coat proteins have been developed that can assemble VLPs. For example, expression of CCMV in *Pichia pastoris* yields up to 0.5 mg per gram of wet cell mass [6]. Heterologous expression in yeast allows large-scale production of wild-type and genetically modified capsids or VLPs. The main advantage of heterologous expression is that it allows production of VLPs that would be unlikely to assemble and accumulate in the natural host cells.

The structure of the wild-type and swollen forms of CCMV has been determined to 3.2 Å [43]. The exterior CCMV capsid electrostatic interactions are well studied [44]. These interactions provide a reversible method to control the assembled capsid structure. The native form of CCMV swells at a pH > 6.5 resulting in 60 pores of 2 nm in size, Figure 6, [2, 44, 45]. The native genetic material can escape via the open pores leaving an empty nano-container for the mineralization of polyoxometalate species, encapsulation of anionic polymers [2, 14] and the synthesis of gold nanoparticle cores [46].

The self-assembly of a virus is initiated by electrostatic interactions between RNA and the protein subunits. In the case of CCMV, mixing the coat protein monomers with different sized polystyrenesulfonate (PSS) polymer to mimic the RNA resulted in two different size morphologies: 22 nm-sized particles generated by using PSS with molecular weight below 2 MDa and 27 nm-sized particles with PSS of 2 MDa or higher [47]. CCMV can also be used for the synthesis of biohybrid nanostructures. It can be self-assembled with a polyethylene glycol (PEG) functionalised exterior surface and can then internalise PSS; expanding the possibilities for new types of hybrid virus nanomaterials [48]. In related work, Hibiscus chlorotic ringspot virus (HCRSV) particles have been used to encapsulate negatively charged polymers including PSS and polyacrylic acid. Reassembly yielded VLPs encapsulating the polymers. However, attempts to encapsulate neutral molecules such as fluorescein-labelled dextran failed, suggesting the encapsulation is based on electrostatic interactions [49].

Material encapsulation into assembled CCMV particles has been an active area of research. For example, the encapsulation of anionic polyanetholesulfonic acid (PASA) is controlled by pH-dependent gating of the CCMV pores [14]. Further, the entrapment of lanthanide ions [14] has been described. A similar approach has been adopted to infuse fluorescent dyes and drugs within RCNMV [50].

### ***Figure 6***

The mineralization reaction within CCMV is electrostatically driven. The interior is highly positively charged and therefore provides an interface for inorganic nucleation. The negatively charged tungstate,  $\text{WO}_4^{4-}$ , and vanadate,  $\text{VO}_3^{3-}$ , anions interact with the interior capsid surface via electrostatic interactions [14]. The same principle was used to generate internalised titanium oxide ( $\beta\text{-TiO}_2$ ) [51] and Prussian blue nanoparticles [52]. Furthermore, the substitution of all the basic residues on the N-terminus of the coat protein with negatively

charged glutamic acid [6] resulted in the mutant favouring interaction with ferrous and ferric ions leading to the formation of magnetite ( $\gamma\text{-Fe}_2\text{O}_3$ ) within the capsid [2].

### 5 Cowpea mosaic virus (CPMV)

CPMV is a non-enveloped plant mosaic virus which is the type member of the comovirus genus of the family Comoviridae [53]. The virus is normally propagated in *Vigna unguiculata*, commonly known as cowpeas or black-eyed peas or beans. In the laboratory, the virus is introduced into the plant by means of mechanical inoculation, which results in mosaic and yellowing symptoms of the leaves. CPMV is considered one of the best investigated viruses and is widely used in bionanotechnology [54, 55]. CPMV capsids have pseudo T=3 icosahedral symmetry and a diameter of approximately 28 nm. The CPMV capsid structure comprises 60 small coat proteins (S, domain A) which folds into one jelly roll  $\beta$ -sandwich arranged as 12 pentamers at the 5-fold axis and 60 large coat proteins (L, domains B and C) arranged as trimers at the 3-fold axis and fold into two jelly roll  $\beta$ -sandwich domains. The three domains form the asymmetric unit. The crystal structure is known to 2.8 Å resolution, Figure 7 [56]. CPMV is a single-stranded positive-sense bipartite RNA virus. Both of the separately encapsidated RNA segments are required for infection [57-59]. However, it was later demonstrated that RNA-1 is independently capable of replicating CPMV particles in protoplasts [60]. RNA-1 encodes the virus replication machinery as well as the virus proteinase and the virus protein genome-linked (VPg), which plays an essential role in initiating RNA synthesis. On the other hand, the smaller RNA-2 encodes the movement protein and the two capsid proteins.

#### **Figure 7**

CPMV particles produced during the infection process can be separated into three components on caesium chloride density gradients. These have identical protein compositions, but differ in their RNA contents [57]. The three centrifugal components are

termed top (T), middle (M), and bottom (B) and contain no RNA, RNA-2, and RNA-1, respectively, Figure 8 [57, 58, 61]. The three components generated during CPMV infection also exist as two electrophoretic forms, slow and fast, Figure 8 [62, 63]. The slow form can be converted to the fast form by proteolytic cleavage at the carboxyl (C)-terminus of the S protein [64, 65]. The conversion occurs naturally during infection, with the fast (C-terminally processed) form of the S protein predominating at later times [64]. Cleavage of the S protein was shown to occur after leucine189 resulting in the loss of the carboxyl-terminal 24 amino acids [10, 66].

### ***Figure 8***

Wild-type CPMV was first mineralized after appropriate genetic modification that involved the use of infectious cDNA clones to modify the capsid, thereby allowing the presentation of foreign peptides on the external CPMV surface [67-69]. It had been established that additional amino acids can be inserted into the highly surface exposed  $\beta$ B- $\beta$ C loop of the small subunit of CPMV. CPMV-based chimaeric virus technology was then adapted for the environmentally benign synthesis of virus-templated monodisperse silica [3] and amorphous iron-platinum nanoparticles [4]. To avoid the lengthy process of generating chimaeric CPMV particles, and to avoid some of the disadvantages of the genetic engineering route (stability, reversion to wild-type and time taken), the possibility of chemically attaching peptides that promote specific mineralization to the surface of CPMV particles was investigated. Peptides previously identified by using phage display that specifically direct mineralization by CoPt (Cbz-CNAGDHANC), FePt (Cbz-HNKHLPSTQPLA), and zinc sulfide (Cbz-CNNPMHQNC) were selected [70, 71] and chemically coupled to the surface exposed lysines, the <sup>Peptide</sup>CPMV was subsequently incubated with the corresponding metal salt and reductant to generate CoPt-CPMV, FePt-CPMV and ZnS-CPMV [72].

The electroless deposition (ELD) method was developed as an alternative approach to generate metal coated virus particles based on the interaction of the CPMV surface amine groups with palladium ions acting as activator sites, which then formed palladium clusters after treatment with a reducing agent (dimethylamine borane). The clusters acted as nucleation sites for the subsequent adsorption of metal ions of interest to generate metal (nickel, cobalt, platinum, iron, nickel-iron, cobalt-platinum) coated CPMV particles. This allowed production of metallized CPMV nanoparticles with a size of 35 nm in diameter; although deposition time could be extended to produce larger metallized spheres [73].

Furthermore, and importantly, it was subsequently shown that there is no requirement for the use of mineral/metal specific peptides or the electroless deposition process for the CPMV-templated formation of monodisperse mineralized nanoparticles; it is sufficient to simply increase the virus surface negative charge. This is done by chemical modification of CPMV surface lysines with succinic acid to increase the overall negative charge on the virus capsid. The charge-modified CPMV, (<sup>Succinamate</sup>CPMV), was coated with cobalt or iron oxide to give monodisperse nanoparticles of about 32 nm diameter. The iron oxide-CPMV nanoparticle surface can be functionalised further with, for example, oligosaccharides [74].

When a cationic polyelectrolyte, poly(allylamine) hydrochloride (PAH), was electrostatically adsorbed onto the external surface of the CPMV capsid. The polyelectrolyte promotes the adsorption of anionic gold complexes, which were then easily reduced, under mild conditions, to form a metallic gold layer. The process is simple and environmentally friendly, as only aqueous solvent and ambient temperature and pressure are required. This route offers a way to produce Au-CPMV with a narrow size distribution which can be further modified with thiol containing moieties [75]. In contrast, reaction of polyelectrolyte-modified CPMV (<sup>PA</sup>CPMV) with pre-formed gold nanoparticles resulted in the self-assembly of large, hexagonally packed, tessellated-spheres, Figure 9 [75].

**Figure 9**

Small lanthanide molecules have been infused and entrapped inside the wild-type CPMV cavity by taking advantage of the negatively charge RNA interaction with gadolinium(III),  $Gd^{3+}$ , and terbium(III),  $Tb^{3+}$ , cations; approximately 80  $Gd^{3+}$  or  $Tb^{3+}$  ions can be encapsulated [76]. However, as the importance of VLPs became apparent, some attempts to inactivate or eliminate the virus RNA within CPMV capsids were reported, including UV irradiation (254 nm) using a dosage of  $2.0 - 2.5 Jcm^{-2}$ . The inactivated particles were deemed as non-infectious to plants. However, particles remained intact and maintained chemical reactivity [77]. Moreover, the RNA content remains encapsidated so that the internal cavity of the particles is not accessible for material loading. Alternatively, alkaline hydrolysis was used to generate artificial empty CPMV particles [9]. The majority of the particles remain intact during the disassembly step. In addition, these processes risk altering the structural properties of the particles and generally do not actually remove RNA from the particles. The recent development of a method for the production of large quantities of CPMV VLPs in plants, as described above [10], was the motivation behind the exploration of loading the generated CPMV VLPs with metal and metal oxide [78], dyes and drugs [79]. It was noticed that the efficiency of loading with metal proved to be variable and depended on the particular VLP preparation used. The role of the carboxyl (C) terminus of the small coat (S) protein in controlling access to the interior of the VLP has been investigated through the determination of the efficiency of internal mineralization with cobalt [63]. The presence of a C-terminal 24-amino acid peptide of the S protein was found to inhibit internal loading, an effect that could be eliminated by enzymatic removal of this region with chymotrypsin. The amenability of the C-terminus to genetic modification has also been demonstrated. Substitution with six histidine residues generated stable particles and facilitated external mineralization by cobalt, Figure 10, [63].

**Figure 10**

## 6 Modifying the virus surface

The virus capsid surface can be addressed with a range of biological and chemical moieties. By doing so, a selection of functionalised nanobuilding blocks can be obtained. The external capsid surface of CCMV, CPMV and TYMV possess a large number of selectively addressable amino acids allowing decoration with a large number of molecules. The native viruses display amine groups, from lysine, and carboxylate groups derived from aspartic and glutamic acids. These functional groups ( $-\text{NH}_2$  or  $-\text{COOH}$ ) on the surface offer a precise addressable site and are the most frequently used for chemical modification. This can be achieved using various techniques of covalent coupling [54, 80-85] and by “click”-chemistry, the copper(I)-catalysed azide-alkyne [3+2] cycloaddition reaction [86-89]. Both wild-type and genetic variants of CPMV have been used as scaffolds for chemical modification; early investigations of the chemical reactivity of wild-type CPMV were aimed at lysine- and cysteine-selective derivatives. The X-ray structure and coordinates of CPMV indicated the presence of five solvent-exposed lysines per asymmetric unit, which equates to 300 exposed lysine side chains per CPMV particle, Figure 11 [90]. In a study on CPMV, single, double, triple, and quadruple lysine-minus mutants, in which the addressable lysines were sequentially replaced with arginines, were generated and chemical labelling efficiency was measured. The studies indicated that all of the five lysines are available for functionalisation; the degree of labelling efficiency varies between the different sites, and normally only four per subunit are modified [83, 91]. The most reactive groups were found to be lysine 38 on the S protein and lysine 99 on the L protein [90].

Carboxylates derived from aspartic and glutamic acids have also been utilised. Chemical attachment of amine-containing compounds can be achieved by making use of the coupling reagents 1-ethyl-3-(3-dimethylaminopropyl) carbodiimide and *N*-hydroxysuccinimide. Up to 180 surface addressable carboxylates per CPMV virion have been modified with different moieties [83, 92]. The native CPMV also displays two surface tyrosines per asymmetric unit

that are available for chemical conjugation [80]. For CCMV around 540 lysine residues and up to 560 carboxylates can be decorated [93]. In the case of TYMV, approximately 60 surface lysines and 90–120 carboxylate groups can be addressed [94].

Thiols derived from cysteine side chains are typically not found in a reactive form on the solvent-exposed surface of viruses; although, cysteine side chains have been identified on the interior solvent-exposed surface of CPMV [86, 95]. As thiols are nevertheless a useful group to use for conjugation a range of cysteine-mutant viruses have been generated via genetic modification [8, 95-101]. For CCMV<sub>CYS</sub> mutant about 100 of the 300 introduced cysteinate-thiols can be labelled [93], for CPMV<sub>CYS</sub> mutant 60 cysteinate-thiols are introduced and addressed [95, 102]. As an alternative route to genetic modification for the introduction of thiol groups at the capsid surface a chemical method has been reported [103]. If required, histidines can be genetically engineered into the external surface [104].

### ***Figure 11***

The phenolic group of tyrosine side chains also provides a possible target for chemical modification. However, the phenolic group is only moderately reactive and to achieve conjugation the tyrosine has to be oxidised by one electron with, for example, peracid or persulfate reagents [105]. Commercial reagents are typically not available; therefore, the starting materials and coupling reagents must be chemically synthesised. The most common reaction utilising tyrosine side chains on viruses is diazonium coupling and this has been widely used with MS2 and TMV [106, 107]. CPMV particles display two accessible tyrosine side chains located in the S subunit, which are available for chemical modification; fluorescein has been covalently attached [80].

CPMV has been utilised to construct enzyme-modified functional virus particles. The well-studied enzymes horseradish peroxidase (HRP) and glucose oxidase (GOX) were employed to

prepare <sup>Enzyme</sup>CPMV conjugates by their conjugation to the external surface of wild-type CPMV. These relatively large biomacromolecules can be bound to the virus surface by simple coupling strategies without destroying their biological activity. The number of enzymes bound to the surface of the virus was determined to be approximately 11 HRP and 2-3 GOX, respectively. The <sup>HRP</sup>CPMV and <sup>GOX</sup>CPMV particles have potential uses as building blocks for catalytic devices, diagnostic assays or biosensors [108].

### ***Figure 12***

In this context, both carboxy- and amine-containing surface exposed amino acids have been modified with electroactive moieties. The incorporation of ferrocene to CPMV (<sup>Ferrocene</sup>CPMV) provided nanostructures with well-defined sizes and functionalities [91]. Cyclic voltammetry established that <sup>Ferrocene</sup>CPMV are redox-active nanoparticles. The ratio of the peak currents is close to unity showing the ferrocene/ferrocenium couple is electrochemically reversible. The peak currents were proportional to the square root of the scan rate indicating that oxidation and reduction were diffusion controlled [83, 91]. Ferrocene dendrimers have shown similar properties due to fast rotation of the dendrimer compared to the electrochemical timescale, so that all the redox centres come close to the electrode within this timescale [109].

Over the past few years a large number of biological, organic and inorganic molecules have been attached to, especially, wild-type CPMV and mutant virions for different applications [110-112], demonstrating that these, and other virus nanoparticles, can be regarded as robust and multi-addressable nanobuilding blocks. In a similar fashion to that described for the icosahedral viruses, TMV has been used as a scaffold for the selective attachment of fluorescent dyes and other small molecules. The native virions offer addressable exterior tyrosine residues and interior carboxylates derived from glutamic acid residues [113]. The tyrosine residues can be quantitatively functionalised with an alkyne residue by diazonium-

coupling, then subsequently copper(I)-catalysed azide-alkyne click-chemistry facilitates the efficient conjugation of a wide range of compounds [114].

## 7 Films, layers and arrays

The formation of highly ordered nanostructured films, layers and arrays are of great interest for the design of novel functional materials that might find applications in, for example, sensors, optoelectronics, nanoelectronics and biomedical applications. Virus nanoparticles have the capability to self-assemble into discrete particles but show also a propensity for self-organisation.

Virus crystallisation can lead to the formation of mesoscale self-organisation in three-dimensions. Icosahedral CPMV particles, for example, can crystallise into well-ordered arrays of  $1 \times 10^{13}$  particles in a typical  $1 \text{ mm}^3$  crystal [102]. CPMV will also self-assemble at the interface between two immiscible liquids. The virus particles segregate at a perfluorodecalin-water interface and stabilise the dispersion of the oil droplets. Cross-linking of the particles at the oil-water interface can be achieved with either glutaraldehyde or with biotin/avidin, which locks the assembly into place to give a well-defined, robust membrane; the integrity of the virus particles are not disrupted [115]. CPMV particles can also be assembled with polyamic acid in aqueous solution via the layer-by-layer technique. Then, upon thermal treatment CPMV particles are removed and polyamic acid is converted into polyimide in one step, resulting in a porous polyimide film [116].

CPMV has been chemically engineered to generate a solvent-free liquid virus, Figure 13 [117]. The CPMV capsid asymmetric unit contains 51 acidic acid residues (21 glutamic acid and 30 aspartic acid). The high anionic charge density was exploited to produce stoichiometric constructs capable of undergoing thermally induced melting in the absence of water. CPMV was cationised by covalent coupling of ethylenediamine. The cationic-CPMV was further modified with anionic polymer-surfactant, poly(ethyleneglycol) 4-nonylphenyl 3-

sulfopropyl ether. Extensive lyophilisation of the single component polymer-surfactant/virus, [Cat-CPMV][S], produced a low-density white solid that on thermal annealing melted to a viscous translucent fluid that on cooling gave a soft, translucent solid. The ability to prepare solvent-free liquids comprising extremely high concentrations of structurally and functionally intact virus nanoparticles should have a significant impact in advancing the bioinspired design and processing of biologically derived nanostructures [117].

### ***Figure 13***

CCMV carries a negative net charge on its outer surfaces at neutral pH (isoelectric point,  $pI \approx 3.8$ ). The negative charge density on CCMV is not homogeneously distributed but is located in patches on the capsid surface. The presence of directional ‘sticky patches’ can direct nanostructure formation, which is controlled by interactions between the patches [118]. 1-Pentanethiol-stabilised gold nanoparticles (AuNPs) were mixed with the virus in different pH conditions that resulted in various patterns of gold super-lattices adsorbed onto the virus capsid [119]. TMV is adsorbed as a monolayer on gold surfaces or hydroxyl containing surfaces, such as mica glass and silicon. In addition, covalent immobilisation can be achieved utilising acyl chloride that reacts with groups on the virus particles to form ester bonds [120]. Genetically modified CCMV<sub>CYS</sub> and CPMV<sub>CYS</sub> VNPs which present cysteine-residues on the surface, can be readily coupled to patterned gold templates using gold-thiol chemistry [96, 121]. Combined with nanolithography techniques this approach was utilised to control assembly of VNPs [121, 122]. A similar method enables the deposition of a uniform monolayer of CPMV<sub>CYS</sub> mutant particles onto a gold surface; this can be visualised by fluorescence microscopy when a suitable dye is conjugated to the virus particles [123]. Alternatively, biotinylated-CPMV can be bound easily to streptavidin (SAv) modified surfaces [123]. Further, CPMV<sub>HIS</sub> mutants, that have introduced histidines onto the solvent exposed surface, have been discretely immobilised on a NeutrAvidin functionalised surface utilising a biotin linker [124]. CPMV<sub>HIS</sub> can also be reversibly coupled to a nickel-

nitriilotriacetic acid-terminated nanografted-patterned surface. The attachment/detachment of the CPMV<sub>HIS</sub> is tuneable by variation of conditions such as pH or addition of imidazole. This system has provided a means of defining the morphological and assembly kinetics of the entropic virus condensation and organisation on the surface as a function of virus flux/mobility and inter-virus interaction [125].

Both CCMV [126] and CPMV [123, 127] 3-dimensional arrays of VNPs were assembled via a layer-by-layer approach using the high affinity interaction between biotin and SA<sub>v</sub>. In the case of CCMV, a monolayer of biotinylated-CCMV was electrostatically conjugated to a functionalised silicon solid surface [44] and then further layers added [126]. For CPMV, the base layer was formed by immobilisation by either direct binding of CPMV<sub>CYS</sub> particles onto gold or indirectly using CPMV-biotin mediated by a thiol-modified SA<sub>v</sub>. For ease of monitoring and tracking the assembly of the layers, one set of virus particles was labelled with the fluorescent dye AlexaFluor (AF) 488 and biotin and the another batch with AF568 and biotin. The first layer of building blocks was assembled with great control using the sulfur-gold interaction (SA<sub>v</sub>-thiol) and further layers by specific interactions between CPMV-bound-biotin and SA<sub>v</sub> [123]. The successful assembly process was monitored by fluorescence microscopy and quartz crystal microbalance with dissipation monitoring [127].

Multilayer structures can also be fabricated by the use of electrostatic interactions. The electrostatic deposition of oppositely charged polyelectrolyte (polyallylamine and polystyrenesulfonate) layers on spherical CarMV particles enabled the polyanion layer to be replaced by a monolayer of negatively charged CarMV particles [128]. The virus was electrostatically adsorbed onto the positively charged polymer and embedded within it. The next deposited layers, of several alternating polyanion and polycation layers, fills holes between the virus and restores the surface layer enabling another layer of virus to be deposited, Figure 14. The electrostatic interaction of CCMV with various surfaces was also investigated [44] led to the construction of alternating polyelectrolyte (polylysine) and CCMV

layers [126]. In this case, a cationic polymer layer was sufficient to promote the binding of successive layers of CCMV. The layer-by-layer approach has also been used to assemble CPMV and TMV into polyelectrolyte substrates [129]. Although CPMV and TMV have similar external surface charge and density, as a consequence of their shape, different layer architectures were obtained. The sphere-like particles are incorporated into the architecture, consistent with the properties of CarMV and CCMV described above, to give a self-assembled, alternating structure of polyelectrolytes and VNPs. However, in stark contrast, the rod-shaped particles are excluded from the arrays and float on top of the polyionic layer architecture in an ordered state. This may provide a starting point for the design and construction of highly organised virus assemblies bound on polyelectrolyte films.

#### ***Figure 14***

TMV can be organised and aligned by an alternative slow assembly technique, by pulling a meniscus containing the virus suspension over a solid surface, to give a film of controlled structure, thickness and long-range virus orientation [130]. The propensity of TMV, at high concentration, to self-assemble into a nematic liquid crystal has been exploited to prepare mesostructured and mesoporous inverse silica replicas, by controlled sol-gel condensation of silicon dioxide on TMV liquid crystals followed by thermal degradation (calcination) [130, 131]. Successful replication of the nematic phase requires balancing the rate of organosilane reagent hydrolysis and the time for realignment of the TMV after initial mixing. The highly ordered, micrometre-sized mesostructures that were obtained consist of a periodic array of co-aligned, end-to-end joined, TMV particles intercalated with a continuous filament of amorphous silica with a periodicity of about 20 nm. Calcination to remove the TMV liquid crystal template has a minimal effect on the periodicity of the inverse replica. At lower reagent concentrations different nanoparticle forms are obtained that, after calcination, have a dense silica core of about 35 nm surrounded by a radial array of linear channels of about 50 nm length [131].

## 8 Applications of viruses in nanotechnology

The use of viruses in nanotechnology offers the prospect of rich and diverse technological advancements. For example, the deposition of platinum on the TMV capsid surface forms nanoparticles with an average diameter of 10 nm [30]. When Pt-TMV was placed between two aluminium electrodes, a unique memory effect was observed in which the RNA and the TMV capsid acted as charge donor and energy barrier, respectively. When a current was applied, the charge transferred from aromatic rings, such as guanine in the RNA, and was trapped in the platinum nanoparticles. The reversible charge transfer and charge trapped process have created a memory device. Similarly, another memory device was designed using CPMV with the exterior capsid modified with quantum dots (QD) [132]. The zinc sulfide capped layer of QD acted as charge storage while the aromatic residues (tryptophan) on the CPMV capsid acted as a charge transport. Ferromagnetic materials play an important role in the development of high-density storage devices, e.g. a computer disk contains a two-dimensional ferromagnetic thin film, where information is stored. Ferromagnetic nanoparticles, like FePt and CoPt [133], have emerged as potential high-density storage media. Therefore, the ability to generate highly monodisperse FePt- and CoPt-CPMV might be an alternative route to synthesise this type of particle [72], although their physical properties are yet to be established. Many VNPs are used to synthesise magnetic and metallic nanoparticles of various shapes. Besides, hollow metallic nanoparticles and nanoshells, which can differ in their properties, might hold great potential in nanomaterial development.

Furthermore, viruses are considered as naturally biocompatible and biodegradable, which is particularly important for medical applications. Plant viruses are less likely to interact with human receptors and virus replication or gene expression is not supported in mammalian systems [85,134]. Nanoparticles and VNPs are currently under investigation in the field of nanomedicine (broadly defined as the application of nanotechnology to medicine) with the aim of control of drug delivery, targeting of diseased cells and as imaging agents. VNPs are

less likely to interact specifically with the mammalian system and, therefore, are less likely to cause potential side effects [135]. For CPMV, it was shown that, even up to dosages of  $10^{16}$  CPMV particles/kg body weight, no apparent toxic side effects were observed in mice [136]. It has been reported that CPMV and CCMV have a broad biodistribution and were detected in a wide variety of tissues throughout the body with no apparent toxic effects [137, 138]. CPMV particles mostly accumulated in the liver and spleen [136]. To reduce their immunogenicity, VNPs can be PEGylated (modified with polyethylene glycol, PEG) [139-141].

VNPs have been modified with fluorophores, quantum dots and metallic nanoparticles, and gadolinium complexes have been developed for *in vivo* imaging agents [105,110, 142, 143]. Fluorescent CPMV particles allowed high-resolution imaging of major blood vessels to a depth of up to 500  $\mu\text{m}$  in comparison to fluorescent-labelled nanospheres [139]. Furthermore, it has been shown that  $\text{Gd}^{3+}$  can be covalently attached to the exterior or interior surface of viruses or electrostatically interacted with the encapsidated RNA molecules [76,144-146] indicating that VNPs could serve as excellent candidates for magnetic resonance imaging (MRI) contrast agents.

To conclude, in this Chapter it has been described how plant viruses can be utilised for the assembly of a wide range of bionanomaterials. The virus particles can be modified on their external surface can incorporate material within their capsids, can form films, layers, arrays and liquid proteins. The potential for their application is extensive, ranging from new materials through novel nanodevices to medical imaging and therapy.

## References

1. Harrison, S. C. (1990). Principles of virus structure in *Fundamental Virology*. NY, Raven Press.
2. Liepold, L. O., J. Revis, M. Allen, L. Oltrogge, M. Young, T. Douglas (2005). Structural transitions in Cowpea chlorotic mottle virus (CCMV). *Physical Biology* 2(4): S166-172.
3. Steinmetz, N. F., N. S. Shah, J. E. Barclay, G. Rallapalli, G. P. Lomonosoff, D. J. Evans (2009). Virus-templated silica nanoparticles. *Small* 5(7): 813-816.
4. Shah, S. N., N. F. Steinmetz, A. A. A. Aljabali, G. P. Lomonosoff, D. J. Evans (2009). Environmentally benign synthesis of virus-templated, monodisperse, iron-platinum nanoparticles. *Dalton Transactions*, 40: 8479-8480.
5. Wellink, J. (1998). Comovirus isolation and RNA extraction. *Methods in Molecular Biology* 81: 205-209.
6. Brumfield, S., D. Willits, L. Tang, J. E. Johnson, T. Douglas, M. Young (2004). Heterologous expression of the modified coat protein of Cowpea chlorotic mottle bromovirus results in the assembly of protein cages with altered architectures and function. *Journal of Genetic Virology* 85(4): 1049-1053.
7. Johnson, J. E. and W. Chiu (2000). Structures of virus and virus-like particles. *Current Opinion in Structural Biology* 10(2): 229-235.
8. Miller, R. A., A. D. Presley, M. B. Francis (2007). Self-assembling light-harvesting systems from synthetically modified tobacco mosaic virus coat proteins. *Journal of the American Chemical Society* 129(11): 3104-3109.
9. Ochoa, W. F., A. Chatterji, T. W. Lin, J. E. Johnson (2006). Generation and structural analysis of reactive empty particles derived from an icosahedral virus. *Chemistry & Biology* 13(7): 771-778.
10. Saunders, K., F. Sainsbury, G. P. Lomonosoff (2009). Efficient generation of Cowpea mosaic virus empty virus-like particles by the proteolytic processing of precursors in insect cells and plants. *Virology* 393(2): 329-337.

11. Sainsbury, F. and G. P. Lomonossoff (2008). Extremely high-level and rapid transient protein production in plants without the use of viral replication. *Plant Physiology* 148(3): 1212-1218.
12. Sainsbury, F., E. C. Thuenemann, G. P. Lomonossoff (2009). pEAQ: versatile expression vectors for easy and quick transient expression of heterologous proteins in plants. *Plant Biotechnology Journal* 7(7): 682-693.
13. Montague, N. P., E. C. Thuenemann, P. Saxena, K. Saunders, P. Lenzi, G. P. Lomonossoff (2011). Recent advances of Cowpea mosaic virus-based particle technology. *Human Vaccine* 7(3): 383-390.
14. Douglas, T. and M. Young, (1998). Host-guest encapsulation of materials by assembled virus protein cages. *Nature* 393(6681): 152-155.
15. Shenton, W., T. Douglas, M. Young, G. Stubbs, S. Mann (1999). Inorganic-organic nanotube composites from template mineralization of tobacco mosaic virus. *Advanced Materials* 11: 253-256.
16. Anobom, C. D., S. C. Albuquerque, F. P. Albernaz, et al. (2003). Structural studies of MS2 bacteriophage virus particle disassembly by nuclear magnetic resonance relaxation measurements. *Biophysical Journal* 84(6): 3894-3903.
17. Abbing, A., U. K. Blaschke, S. Grein, et al. (2004). Efficient intracellular delivery of a protein and a low molecular weight substance via recombinant polyomavirus-like particles. *Journal of Biological Chemistry* 279(26): 27410-27421.
18. Douglas, T. and M. Young (1999). Virus particles as templates for materials synthesis. *Advanced Materials* 11(8): 679-681.
19. Comellas-Aragones, M., H. Engelkamp, V. I. Claessen, et al. (2007). A virus-based single-enzyme nanoreactor. *Nature Nanotechnology* 2(10): 635-639.
20. Loo, L., R. H. Guenther, V. R. Basnayake, S. A. Lommel, S. Franzen (2006). Controlled encapsidation of gold nanoparticles by a viral protein shell. *Journal of the American Chemical Society* 128(14): 4502-4503.

21. Loo, L., R. H. Guenther, S. A. Lommel, S. Franzen (2007). Encapsulation of nanoparticles by Red clover necrotic mosaic virus. *Journal of the American Chemical Society* 129(36): 11111-11117.
22. Dragnea, B., C. Chen, E. S. Kwak, B. Stein, C. C. Kao (2003). Gold nanoparticles as spectroscopic enhancers for in vitro studies on single viruses. *Journal of the American Chemical Society* 125(21): 6374-6375.
23. Chen, C., M. C. Daniel, Z. T. Quinkert, et al. (2006). Nanoparticle-templated assembly of viral protein cages. *Nano Letters* 6(4): 611-615.
24. Dixit, S. K., N. L. Goicochea, M. C. Daniel, et al. (2006). Quantum dot encapsulation in viral capsids. *Nano Letters* 6(9): 1993-1999.
25. Pattanayek, R. and G. Stubbs (1992). Structure of the U2 strain of tobacco mosaic virus refined at 3.5 Å resolution using X-ray fiber diffraction. *Journal of Molecular Biology* 228(2): 516-528.
26. Stubbs, G. (1999). Tobacco mosaic virus particle structure and the initiation of disassembly. *Philosophical Transactions of the Royal Society of London Series B-Biological Sciences* 354(1383): 551-557.
27. Balci, S., A. M. Bittner, M. Schirra, et al. (2009). Catalytic coating of virus particles with zinc oxide. *Electrochimica Acta* 54(22): 5149-5154.
28. Knez, M., A. Kadri, C. Wege, U. Gosele, H. Jeske, K. Nielsch (2006). Atomic layer deposition on biological macromolecules: Metal oxide coating of tobacco mosaic virus and ferritin. *Nano Letters* 6(6): 1172-1177.
29. Royston, E., S. Y. Lee, J. N. Culver, M. T. Harris (2006). Characterization of silica-coated tobacco mosaic virus. *Journal of Colloid and Interface Science* 298(2): 706-712.
30. Gorzny, M. L., A. S. Walton, M. Wnek, P. G. Stockley, S. D. Evans (2008). Four-probe electrical characterization of Pt-coated TMV-based nanostructures. *Nanotechnology* 19(16):165704.

31. Liu, N., C. Wang, W. Zhang et al. (2012). Au nanocrystals grown on a better-defined one-dimensional tobacco mosaic virus coated protein template genetically modified by a hexahistidine tag. *Nanotechnology* 23(33): 335602.
32. Wnek, M., M. L. Gorzny, M. B. Ward et al. (2013). Fabrication and characterization of gold nano-wires templated on virus-like arrays of tobacco mosaic virus coat proteins. *Nanotechnology* 24(2): 025605.
33. Rong, J. H., F. Oberbeck, X. N. Wang, et al. (2009). Tobacco mosaic virus templated synthesis of one dimensional inorganic-polymer hybrid fibres. *Journal of Materials Chemistry* 19(18): 2841-2845.
34. Balci, S., K. Hahn, P. Kopold, et al. (2012). Electroless synthesis of 3 nm wide alloy nanowires inside tobacco mosaic virus. *Nanotechnology* 23(4): 045603.
35. Lee, S. Y., E. Royston, J. N. Culver, M. T. Harris, (2005). Improved metal cluster deposition on a genetically engineered tobacco mosaic virus template. *Nanotechnology* 16(7): S435-441.
36. Niu, Z., M. A. Bruckman, S. Q. Li et al. (2007). Assembly of tobacco mosaic virus into fibrous and macroscopic bundled arrays mediated by surface aniline polymerization. *Langmuir* 23(12): 6719-6724.
37. Namba, K. and G. Stubbs (1986). Structure of tobacco mosaic virus at 3.6 Å resolution: implications for assembly. *Science* 231(4744): 1401-1406.
38. Dujardin, E., C. Peet, G. Stubbs, J. N. Culver, S. Mann (2003). Organisation of metallic nanoparticles using tobacco mosaic virus. *Nano Letters* 3: 413-417.
39. Bromley, K. M., A. J. Patil, A. W. Perriman, G. Stubbs, S. Mann (2008). Preparation of high quality nanowires by tobacco mosaic virus templating of gold nanoparticles. *Journal of Materials Chemistry* 18: 4796-4801.
40. Knez, M., M. Sumser, A. M. Bittner, et al. (2004). Spatially selective nucleation of metal clusters on the tobacco mosaic virus. *Advanced Functional Materials* 14(2): 116-124.
41. Balci, S., A. M. Bittner, K. Hahn, et al. (2006). Copper nanowires within the central channel of tobacco mosaic virus particles. *Electrochimica Acta* 51(28): 6251-6257.

42. Royston, E., A. Ghosh, P. Kofinas, M. T. Harris, J. N. Culver (2008). Self-assembly of virus-structured high surface area nanomaterials and their application as battery electrodes. *Langmuir* 24(3): 906-912.
43. Speir, J. A., S. Munshi, G. Wang, T. S. Baker, J. E. Johnson (1995). Structures of the native and swollen forms of Cowpea chlorotic mottle virus determined by X-ray crystallography and cryo-electron microscopy. *Structure* 3(1): 63-78.
44. Suci, P. A., M. T. Klem, F. T. Arce, T. Douglas, M. Young (2005). Influence of electrostatic interactions on the surface adsorption of a viral protein cage. *Langmuir* 21(19): 8686-8693.
45. Schneemann, A. and M. J. Young (2003). Viral assembly using heterologous expression systems and cell extracts. *Virus Structure* 64: 1-36.
46. Slocik, J. M., R. R. Naik, M. O. Stone, D. W. Wright (2005). Viral templates for gold nanoparticles synthesis. *Journal of Materials Chemistry* 15(7): 749-753.
47. Hu, Y. F., R. Zandi, A. Anavitarte, C. M. Knobler, W. M. Gelbart (2008). Packaging of a polymer by a viral capsid: The interplay between polymer length and capsid size. *Biophysical Journal* 94(4): 1428-1436.
48. Comellas-Aragones, M., A. de la Escosura, A. J. Dirks, et al. (2009) Controlled integration of polymers into viral capsids. *Biomacromolecules* 10(11): 3141-3147.
49. Ren, Y. P., S. M. Wong, L. Y. Lim (2006). In vitro-reassembled plant virus-like particles for loading of polyacids. *Journal of General Virology* 87: 2749-2754.
50. Loo, L., R. H. Guenther, S. A. Lommel, S. Franzen (2008). Infusion of dye molecules into Red clover necrotic mosaic virus. *Chemical Communications*(1): 88-90.
51. Klem, M. T., M. Young, T. Douglas (2008). Biomimetic synthesis of  $\beta$ -TiO<sub>2</sub> inside a viral capsid. *Journal of Materials Chemistry* 18: 3821-3823.
52. de la Escosura, A., M. Verwegen, F. D. Sikkema, et al. (2008). Viral capsids as templates for the production of monodisperse Prussian blue nanoparticles. *Chemical Communications* (13): 1542-1544.

53. Lin, T. and J. E. Johnson (2003). Structures of picorna-like plant viruses: implications and applications. *Advances in Virus Research* 62: 167-239.
54. Evans, D. J. (2010). Bionanoscience at the plant virus-inorganic chemistry interface. *Inorganica Chimica Acta* 363(6): 1070-1076.
55. Sainsbury, F., M. C. Cañizares, G. P. Lomonossoff (2010). Cowpea mosaic virus: the plant virus-based biotechnology workhorse. *Annual Review of Phytopathology* 48(1): 437-455.
56. Lin, T. W., Z. G. Chen, R. Usha, et al. (1999). The refined crystal structure of Cowpea mosaic virus at 2.8 Ångstrom resolution. *Virology* 265(1): 20-34.
57. Bruening, G. and H. O. Agrawal (1967). Infectivity of a mixture of Cowpea mosaic virus ribonucleoprotein components. *Virology* 32(2): 306-320.
58. van Kammen, A. (1967). Purification and properties of the components of Cowpea mosaic virus. *Virology* 31(4): 633-642.
59. Liu, L. and G. P. Lomonossoff (2002). Agroinfection as a rapid method for propagating Cowpea mosaic virus-based constructs. *Journal of Virological Methods* 105(2): 343-348.
60. Goldbach, R., G. Rezelman, A. Vankammen (1980). Independent replication and expression of B-component RNA of Cowpea mosaic virus. *Nature* 286(5770): 297-300.
61. Lomonossoff, G. P. and J. E. Johnson (1991). The synthesis and structure of Comovirus capsids. *Progress in Biophysics & Molecular Biology* 55(2): 107-137.
62. Semancik, J. S. (1966). Studies on electrophoretic heterogeneity in isometric plant viruses. *Virology* 30(4): 698-704.
63. Sainsbury, F., K. Saunders, A. A. A. Aljabali, D. J. Evans, G. P. Lomonossoff (2011). Peptide-controlled access to the interior surface of empty virus nanoparticles. *ChemBioChem* 12: 2435-2440.
64. Niblett, C. L. and J. S. Semancik (1969). Conversion of the electrophoretic forms of Cowpea mosaic virus in vivo and in vitro. *Virology* 38(4): 685-693.
65. Kridl, J. C. and G. Bruening (1983). Comparison of capsids and nucleocapsids from Cowpea mosaic virus-infected Cowpea protoplasts and seedlings. *Virology* 129(2): 369-380.

66. Taylor, K. M., V. E. Spall, P. J. G. Butler, G. P. Lomonossoff (1999). The cleavable carboxyl-terminus of the small coat protein of Cowpea mosaic virus is involved in RNA encapsidation. *Virology* 255(1): 129-137.
67. Dessens, J. T. and G. P. Lomonossoff (1993). Cauliflower mosaic virus 35S promoter-controlled DNA copies of Cowpea mosaic virus RNAs are infectious on plants. *Journal of Genetic Virology* 74 (5): 889-892.
68. Lin, T., C. Porta, G. P. Lomonossoff, J. E. Johnson (1996). Structure-based design of peptide presentation on a viral surface: the crystal structure of a plant/animal virus chimera at 2.8 Å resolution. *Folding and Design* 1(3): 179-187.
69. Lomonossoff, G. P. and Johnson, J. E. (1996). Use of macromolecular assemblies as expression systems for peptides and synthetic vaccines. *Current Opinion in Structural Biology* 6(2): 176-182.
70. Mao, C., D. J. Solis, B. D. Reiss et al. (2004). Virus-based toolkit for the directed synthesis of magnetic and semiconducting nanowires. *Science* 303(5655): 213-217.
71. Reiss, B. D., C. Mao, D. J. Solis, K. S. Ryan, T. Thomson, A. M. Belcher (2004). Biological routes to metal alloy ferromagnetic nanostructures. *Nano Letters* 4(6): 1127-1132.
72. Aljabali, A. A. A, S. N. Shah, R. Evans-Gowing, G. P. Lomonossoff, D. J. Evans (2011). Chemically-coupled-peptide-promoted virus nanoparticle templated mineralization. *Integrative Biology* 3(2): 119-125.
73. Aljabali, A. A. A., J. E. Barclay, G. P. Lomonossoff, D. J. Evans (2010). Virus templated metallic nanoparticles. *Nanoscale* 2: 2596-2600.
74. Aljabali, A. A. A., J. E. Barclay, O. Cespedes, et al. (2011). Charge modified Cowpea mosaic virus particles for templated mineralization. *Advanced Functional Materials* 21(21): 4137-4142.
75. Aljabali, A. A. A., G. P. Lomonossoff, D. J. Evans (2011). CPMV-polyelectrolyte-templated gold nanoparticles. *Biomacromolecules* 12(7): 2723-2728.

76. Prasuhn, D. E., Jr., R. M. Yeh, A. Obenaus, M. Manchester, M. G. Finn (2007). Viral MRI contrast agents: coordination of Gd by native virions and attachment of Gd complexes by azide-alkyne cycloaddition. *Chemical Communications* (12): 1269-1271.
77. Rae, C., K. J. Koudelka, G. Destito, M. N. Estrada, M. J. Gonzalez, M. Manchester (2008). Chemical addressability of ultraviolet-inactivated viral nanoparticles (VNPs). *PLoS One* 3(10): e3315.
78. Aljabali, A. A. A., F. Sainsbury, G. P. Lomonosoff, D. J. Evans (2010). Cowpea mosaic virus unmodified empty viruslike particles loaded with metal and metal oxide. *Small* 6(7): 818-821.
79. Wen, A. M., S. Shukla, P. Saxena et al. (2012). Interior engineering of a viral nanoparticle and its tumor homing properties. *Biomacromolecules* 13(12): 3990-4001.
80. Meunier, S., E. Strable, M. G. Finn (2004). Crosslinking of and coupling to viral capsid proteins by tyrosine oxidation. *Chemical Biology* 11(3): 319-326.
81. Hermanson, T. G. (2008). *Bioconjugate Techniques*. London, Academic Press.
82. Laufer, B., N. F. Steinmetz, V. Hong, M. Manchester, H. Kessler, M. G. Finn (2009). Guiding VLP's the right way: coating of virus like particles with peptidic integrin ligands. *Biopolymers* 92(4): 323-323.
83. Aljabali, A. A. A., J. E. Barclay, J. N. Butt, G. P. Lomonosoff, D. J. Evans (2010). Redox-active ferrocene-modified Cowpea mosaic virus nanoparticles. *Dalton Transactions* 39(32): 7569-7574.
84. Pokorski, J. K. and N. F. Steinmetz (2011). The art of engineering viral nanoparticles. *Molecular Pharmaceutics* 8(1): 29-43.
85. Steinmetz, N. F., C. F. Cho, A. Ablack, J. D. Lewis, M. Manchester (2011). Cowpea mosaic virus nanoparticles target surface vimentin on cancer cells. *Nanomedicine* 6(2): 351-364.
86. Wang, Q., T. R. Chan, R. Hilgraf, V. V. Fokin, K. B. Sharpless, M. G. Finn (2003). Bioconjugation by copper(I)-catalyzed azide-alkyne [3 + 2] cycloaddition. *Journal of the American Chemical Society* 125(11): 3192-3193.

87. Sen Gupta, S., J. Kuzelka, P. Singh, W. G. Lewis, M. Manchester, M. G. Finn (2005). Accelerated bioorthogonal conjugation: a practical method for the ligation of diverse functional molecules to a polyvalent virus scaffold. *Bioconjugate Chemistry* 16(6): 1572-1579.
88. Sen Gupta, S., K. S. Raja, E. Kaltgrad, E. Strable, M. G. Finn (2005). Virus-glycopolymer conjugates by copper(I) catalysis of atom transfer radical polymerization and azide-alkyne cycloaddition. *Chemical Communications* (34): 4315-4317.
89. Manchester, M. and P. Singh (2006). Virus-based nanoparticles (VNPs): platform technologies for diagnostic imaging. *Advanced Drug Delivery Review* 58(14): 1505-1522.
90. Chatterji, A., W. Ochoa, M. Paine, B. R. Ratna, J. E. Johnson, T. W. Lin, (2004). New addresses on an addressable virus nanoblock: uniquely reactive Lys residues on Cowpea mosaic virus. *Chemical Biology* 11(6): 855-863.
91. Steinmetz, N. F., G. P. Lomonosoff, D. J. Evans (2006). Decoration of Cowpea mosaic virus with multiple, redox-active, organometallic complexes. *Small* 2(4): 530-533.
92. Steinmetz, N. F., G. P. Lomonosoff, D. J. Evans (2006). Cowpea mosaic virus for material fabrication: addressable carboxylate groups on a programmable nanoscaffold. *Langmuir* 22(8): 3488-3490.
93. Gillitzer, E., D. Willits, M. Young, T. Douglas (2002). Chemical modification of a viral cage for multivalent presentation. *Chemical Communications* (20): 2390-2391.
94. Barnhill, H. N., R. Reuther, P. L. Ferguson, T. Dreher, Q. Wang (2007). Turnip yellow mosaic virus as a chemoaddressable bionanoparticle. *Bioconjugate Chemistry* 18(3): 852-859.
95. Wang, Q., T. Lin, J. E. Johnson, M. G. Finn (2002). Natural supramolecular building blocks. cysteine-added mutants of Cowpea mosaic virus. *Chemical Biology* 9(7): 813-819.
96. Klem, M. T., D. Willits, M. Young, T. Douglas (2003). 2-D array formation of genetically engineered viral cages on Au surfaces and imaging by atomic force microscopy. *Journal of the American Chemical Society* 125(36): 10806-10807.
97. Peabody, D. S. (2003). A viral platform for chemical modification and multivalent display. *Journal of Nanobiotechnology* 1(5).

98. Kreppel, F., J. Gackowski, E. Schmidt, S. Kochanek (2005). Combined genetic and chemical capsid modifications enable flexible and efficient de- and retargeting of adenovirus vectors. *Molecular Therapy* 12(1): 107-117.
99. Khalil, A. S., J. M. Ferrer, R. R. Brau, et al. (2007). Single M13 bacteriophage tethering and stretching. *The Proceedings of the National Academy of Sciences (U.S.A)* 104(12): 4892-4897.
100. Destito, G., A. Schneemann, M. Manchester, et al. (2009). Biomedical nanotechnology using virus-based nanoparticles. *Current Topics of Microbiology and Immunology* 327: 95-122.
101. Blum, A. S., C. M. Soto, C. D. Wilson, et al. (2004). Cowpea mosaic virus as a scaffold for 3-D patterning of gold nanoparticles. *Nano Letters* 4(5): 867-870.
102. Wang, Q., T. Lin, L. Tang, J. E. Johnson, M. G. Finn (2002). Icosahedral virus particles as addressable nanoscale building blocks. *Angewandte Chemie-International Edition* 41(3): 459-462.
103. Steinmetz, N. F., D. J. Evans, G. P. Lomonosoff (2007). Chemical introduction of reactive thiols into a viral nanoscaffold: A method that avoids virus aggregation. *ChemBioChem* 8(10): 1131-1136.
104. Chatterji, A., W. F. Ochoa, T. Ueno, T. W. Lin, J. E. Johnson (2005). A virus-based nanoblock with tunable electrostatic properties. *Nano Letters* 5(4): 597-602.
105. Manchester, M. and N. F. Steinmetz (2009). *Viruses and nanotechnology. Current Topics in Microbiology and Immunology.* Berlin, Heidelberg, Springer.
106. Kovacs, E. W., J. M. Hooker, D. W. Romanini, P. G. Holder, K. E. Berry, M. B. Francis (2007). Dual-surface-modified bacteriophage MS2 as an ideal scaffold for a viral capsid-based drug delivery system. *Bioconjugate Chemistry* 18(4): 1140-1147.
107. Schlick, T. L., Z. Ding, E. W. Kovacs, M. B. Francis (2005). Dual-surface modification of the tobacco mosaic virus. *Journal of the American Chemical Society* 127: 3718-3723.

108. Aljabali, A. A. A., J. E. Barclay, N. F. Steinmetz, G. P. Lomonossoff, D. J. Evans (2012). Controlled immobilisation of active enzymes on the Cowpea mosaic virus capsid. *Nanoscale* 4(18): 5640-5645.
109. Green, S. J., J. J. Pietron, J. J. Stokes, et al. (1998). Three-dimensional monolayers: Voltammetry of alkanethiolate-stabilized gold cluster molecules. *Langmuir* 14(19): 5612-5619.
110. Steinmetz, N. F. and D. J. Evans (2007). Utilisation of plant viruses in bionanotechnology. *Organic & Biomolecular Chemistry* 5(18): 2891-2902.
111. Evans, D. J. (2008). The bionanoscience of plant viruses: templates and synthons for new materials. *Journal of Materials Chemistry* 18(32): 3746-3754.
112. Yildiz, I., S. Shukla, N. F. Steinmetz (2011). Applications of viral nanoparticles in medicine. *Current Opinion Biotechnology* 22(6): 901-908.
113. Young, M., D. Willits, M. Uchida, T. Douglas (2008). Plant viruses as biotemplates for materials and their use in nanotechnology. *Annual Review of Phytopathology* 46: 361-384.
114. Zhang, X. and Y. Zhang (2013). Applications of azide-based bioorthogonal click chemistry in glycobiology. *Molecules* 18(6): 7145-7159.
115. Russell, J. T., Y. Lin, A. Bokeret et al. (2005). Self-assembly and cross-linking of bionanoparticles at liquid-liquid interfaces. *Angewandte Chemie-International Edition* 44(16): 2420-2426.
116. Peng, B., G. J. Wu, Y. Lin, Q. Wang, Z. H. Su (2011). Preparation of nanoporous polyimide thin films via layer-by-layer self-assembly of Cowpea mosaic virus and poly(amic acid). *Thin Solid Films* 519(22): 7712-7716.
117. Patil, A. J., N. McGrath, J. E. Barclay, et al. (2012). Liquid viruses by nanoscale engineering of capsid surfaces. *Advanced Materials* 24(33): 4557-4563.
118. Glotzer, S. C. and M. J. Solomon (2007). Anisotropy of building blocks and their assembly into complex structures. *Nature Materials* 6(8): 557-562.
119. Kostianen, M. A., P. Hiekkataipale, A. Laiho, et al. (2013). Electrostatic assembly of binary nanoparticle superlattices using protein cages. *Nature Nanotechnology* 8(1): 52-55.

120. Knez, M., M. P. Sumser, A. M. Bittner, et al. (2004). Binding the tobacco mosaic virus to inorganic surfaces. *Langmuir* 20(2): 441-447.
121. Smith, J. C., K. B. Lee, Q. Wang, et al. (2003). Nanopatterning the chemospecific immobilization of cowpea mosaic virus capsid. *Nano Letters* 3(7): 883-886.
122. Cheung, C. L., J. A. Camarero, B. W. Woods, T. W. Lin, J. E. Johnson, J. J. De Yoreo, (2003). Fabrication of assembled virus nanostructures on templates of chemoselective linkers formed by scanning probe nanolithography. *Journal of the American Chemical Society* 125(23): 6848-6849.
123. Steinmetz, N. F., G. Calder, R. P. Richter, J. P. Spatz, G. P. Lomonosoff, D. J. Evans (2006). Plant viral capsids as nanobuilding blocks: Construction of arrays on solid supports. *Langmuir* 22(24): 10032-10037.
124. Medintz, I. L., K. E. Sapsford, J. H. Konnert, et al. (2005). Decoration of discretely immobilized Cowpea mosaic virus with luminescent quantum dots. *Langmuir* 21(12): 5501-5510.
125. Cheung, C. L., S. W. Chung, A. Chatterji, et al. (2006). Physical controls on directed virus assembly at nanoscale chemical templates. *Journal of the American Chemical Society* 128(33): 10801-10807.
126. Suci, P. A., M. T. Klem, F. T. Arce, T. Douglas, M. Young (2006). Assembly of multilayer films incorporating a viral protein cage architecture. *Langmuir* 22(21): 8891-8896.
127. Steinmetz, N. F., E. Bock, R. P. Richter, J. P. Spatz, G. P. Lomonosoff, D. J. Evans (2008). Assembly of multilayer arrays of viral nanoparticles via biospecific recognition: a quartz crystal microbalance with dissipation monitoring study. *Biomacromolecules* 9(2): 456-462.
128. Lvov, Y., H. Haas, G. Decher, et al. (1994). Successive deposition of alternate layers of polyelectrolytes and a charged virus. *Langmuir* 10(11): 4232-4236.
129. Steinmetz, N. F., K. C. Findlay, T. R. Noel, R. Parker, G. P. Lomonosoff, D. J. Evans (2008). Layer-by-layer assembly of viral nanoparticles and polyelectrolytes: The film architecture is different for spheres versus rods. *ChemBioChem* 9(10): 1662-1670.

130. Kuncicky, D. M., R. R. Naik, O. D Velev (2006). Rapid deposition and long-range alignment of nanocoatings and arrays of electrically conductive wires from tobacco mosaic virus. *Small* 2(12): 1462-1466.
131. Fowler, C. E., W. Shenton, G. Stubbs, S. Mann (2001). Tobacco mosaic virus liquid crystals as templates for the interior design of silica mesophases and nanoparticles. *Advanced Materials* 13(16): 1266-1269.
132. Portney, N. G., R. J. Tseng, G. Destito, et al. (2007). Microscale memory characteristics of virus-quantum dot hybrids. *Applied Physics Letters* 90(21): 214104.
133. Sun, X. C., Y. H. Huang, D. E. Nikles (2004). FePt and CoPt magnetic nanoparticles film for future high density data storage media. *International Journal of Nanotechnology* 1(3): 328-346.
134. Koudelka, K. J. and M. Manchester (2010). Chemically modified viruses: principles and applications. *Current Opinion in Chemical Biology* 14(6): 810-817.
135. Koudelka, K. J., G. Destito, E. M. Plummer, S. A. Trauger, G. Siuzdak, M. Manchester, (2009). Endothelial targeting of Cowpea mosaic virus (CPMV) via surface vimentin. *PLoS Pathogens* 5(5): e1000417.
136. Singh, P., D. Prasuhn, R. M. Yeh, et al. (2007). Bio-distribution, toxicity and pathology of Cowpea mosaic virus nanoparticles in vivo. *Journal of Controlled Release* 120(1-2): 41-50.
137. Rae, C. S., I. W. Khor, Q. Wang, et al. (2005). Systemic trafficking of plant virus nanoparticles in mice via the oral route. *Virology* 343(2): 224-235.
138. Kaiser, C. R., M. L. Flenniken, E. Gillitzer, et al. (2007). Biodistribution studies of protein cage nanoparticles demonstrate broad tissue distribution and rapid clearance in vivo. *International Journal of Nanomedicine* 2(4): 715-733.
139. Lewis, J. D., G. Destito, A. Zijlstra, et al. (2006). Viral nanoparticles as tools for intravital vascular imaging. *Nature Medicine* 12(3): 354-360.
140. Destito, G., R. Yeh, C. S. Rae, M. G. Finn, et al. (2007). Folic acid-mediated targeting of Cowpea mosaic virus particles to tumor cells. *Chemistry & Biology* 14(10): 1152-1162.

141. Steinmetz, N. F. and M. Manchester (2009). PEGylated viral nanoparticles for biomedicine: the impact of PEG chain length on VNP cell interactions in vitro and ex vivo. *Biomacromolecules* 10(4): 784-792.
142. Singh, P., M. J. Gonzalez, M. Manchester (2006). Viruses and their uses in nanotechnology. *Drug Development Research* 67: 23-41.
143. Steinmetz, N. F., T. Lin, G. P. Lomonossoff, J. E. Johnson (2009). Structure-based engineering of an icosahedral virus for nanomedicine and nanotechnology. *Current Topics of Microbiology and Immunology* 327: 23-58.
144. Allen, M., J. W. Bulte, L. Liepold, et al. (2005). Paramagnetic viral nanoparticles as potential high-relaxivity magnetic resonance contrast agents. *Magnetic Resonance in Medicine* 54(4): 807-812.
145. Anderson, E. A., S. Isaacman, D. S. Peabody, E. Y. Wang, J. W. Canary, K. Kirshenbaum (2006). Viral nanoparticles donning a paramagnetic coat: conjugation of MRI contrast agents to the MS2 capsid. *Nano Letters* 6(6): 1160-1164.
146. Hooker, J. M., A. Datta, M. Botta, K. N. Raymond, M. B. Francis (2007). Magnetic resonance contrast agents from viral capsid shells: a comparison of exterior and interior cargo strategies. *Nano Letters* 7(8): 2207-2210.

## Figure Legends

Figure 1 Space filling representation of some plant viruses. Virus structure was generated from (<http://viperd.b.scripps.edu>). TMV images were taken from (<http://tinyurl.com/nyjmhdj>).

Figure 2 Schematic of potential chemical modification sites of an icosahedral plant virus capsid: external surface, internal surface, internal loading, external coating

Figure 3 Cryoelectron microscopy reconstructions of CPMV particles. Purified particles were flash-frozen in vitreous ice and then subjected to cryoelectron microscopy. (A) reconstruction of wild-type CPMV exterior, (B) reconstruction of CPMV VLPs, (C) internal view of CPMV VLPs showing empty cavity and (D) wild-type CPMV with encapsidated RNA in blue.

Images courtesy of Dr Kyle Dent and Dr Neil Ranson, University of Leeds, United Kingdom.

Figure 4 Assembly of RCNMV VLPs around a gold nanoparticle via OAS templating. (A) conjugation of nanoparticle with DNA-2; (B) addition of RNA-1, which interacts with DNA-2 to form the functional OAS; (C) the artificial OAS templates the assembly of coat protein; and (D) formation of virus-like particle with nanoparticle encapsidated. Reprinted with permission from Loo, et al., J. Am. Chem. Soc. (2006) 128, 4502. Copyright 2006 American Chemical Society.

Figure 5 Proposed mechanism of VLP assembly from coat proteins. (a) Electrostatic interaction leads to the formation of disordered protein-gold nanoparticle complexes. The second step is a crystallization phase in which the protein-protein interactions lead to the formation of a regular capsid. (b) Schematic depiction of the encapsidated nanoparticle functionalised with carboxyl-terminated PEG chains. Right: Cryoelectron micrograph of a single VLP shows the protein structure coating the 12 nm diameter gold nanoparticle (black

disk). Reprinted with permission from Chen, et al., *Nano Letters* (2006) 6, 611. Copyright 2006 American Chemical Society.

Figure 6 Cryoelectron microscopy and image reconstruction of Cowpea chlorotic mottle virus. In an unswollen condition induced by low pH (on the left) and in a swollen condition induced by high pH (on the right). Swelling at the pseudo-three-fold axis results in the formation of sixty 2 nm pores. Reprinted by permission from Macmillan Publishers Ltd: *Nature*, Douglas and Young (1998) 393, 152, Copyright (1998).

Figure 7 The structure of Cowpea mosaic virus (CPMV) capsid and the asymmetric unit. CPMV capsid is comprised of small (S) and large (L) sub-units. The A domain (in blue), B domain (in green) and C domain (in yellow). Adapted from Steinmetz and Evans, *Org. Biomol. Chem.* (2007) 8, 1131 - Reproduced by permission of The Royal Society of Chemistry.

Figure 8 Separation of the different components of Cowpea mosaic virus. (A) In a caesium chloride gradient by ultracentrifugation (B) Electrophoretic travel of particles containing the different forms of the S subunit, the slow (s) and the fast (f). Images in (A) courtesy of Dr. Keith Saunders, John Innes Centre, United Kingdom.

Figure 9 Stained TEM image of a single tessellated-sphere showing the CPMV particles as hexagonally packed mosaic pieces in a spherical arrangement together with gold nanoparticles that appear as black circles. Reprinted with permission from Aljabali, et al., *Biomacromolecules* (2011) 12, 2723. Copyright 2011 American Chemical Society.

Figure 10 Loading of CPMV VLPs with cobalt. (A) Agarose gel of wild-type and LD4His VLPs subjected to the cobalt loading reaction. Wild-type VLPs were subjected to cobalt loading with (+ve) and without (-ve) pre-treatment with chymotrypsin. CPMV virions

(CPMV) and top components (Top) were electrophoresed as controls. The gel was stained with Coomassie brilliant blue. (B) Representation of the pattern of mineralization of VLP variants showing dynamic light scattering measurements taken after the cobalt loading reaction: -ve shows no mineralization, +ve is internally mineralized, and LD4His is externally mineralized. Reprinted with permission from Sainsbury, et al., *ChemBioChem* (2011) 12, 2453. Copyright 2011 Wiley-VCH Verlag GmbH & Co.

Figure 11 Schematic representation of the surface exposed addressable amines and carboxylates of the CPMV capsid. Adapted from Steinmetz and Evans, *Org. Biomol. Chem.* (2007) 8, 1131 - Reproduced by permission of The Royal Society of Chemistry.

Figure 12 TEM image of <sup>HRP-ADH</sup>CPMV particles stained with 1% AgNO<sub>3</sub> solution that stains specifically the generated aldehyde groups as a result of the oxidation process confirming the presence of enzyme. Inset confirms the localization of the metallic silver on the virus capsid. Adapted from Aljabali et al., *Nanoscale* (2012), 4, 5640 - Reproduced by permission of The Royal Society of Chemistry.

Figure 13 Optical photographs of sample tubes containing [Cat-CPMV][S] showing a low density white solid obtained after lyophilization (A) and a highly viscous translucent fluid obtained after annealing the freeze-dried material at 65 °C for 10 minutes (B). (C) Optical image showing single liquid droplet of a solvent-free [Cat-CPMV][S] melt placed on a glass slide at 65 °C. Reprinted with permission from Patil, et al., *Advanced Materials* (2012) 24, 4557. Copyright 2012 Wiley-VCH Verlag GmbH & Co.

Figure 14 The deposition process of alternate layers of polyelectrolytes and Carnation mottle virus (CarMV). (a) Smooth polyelectrolyte precursor film. (b) Adsorbed virus particles partially intrude into the polymer layer. (c) The next polymer layer fills the empty space between the viruses and leads to a partial annealing of the surface. (d) Further polymer layers

completely anneal the surface so as to give conventional roughness and layer thickness.

Reprinted with permission from Lvov et al., *Langmuir*, (1994), 10, 4232. Copyright 1994

American Chemical Society.

### Figures.

Figure 1.

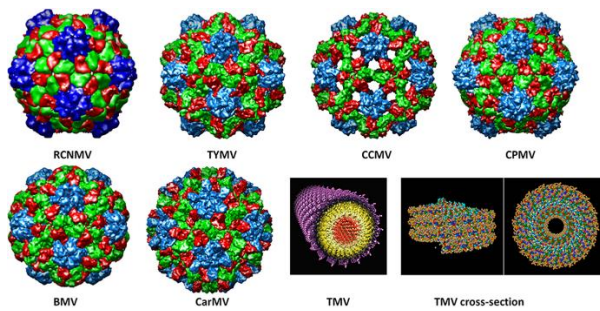


Figure 2.

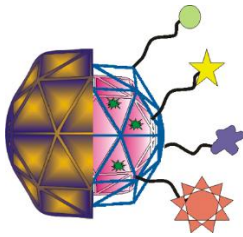


Figure 3.

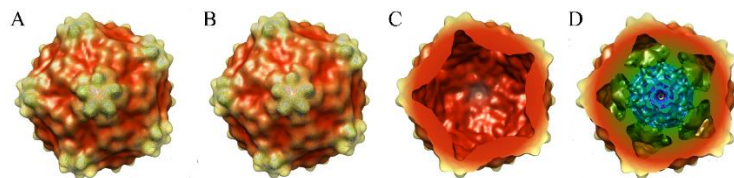


Figure 4.

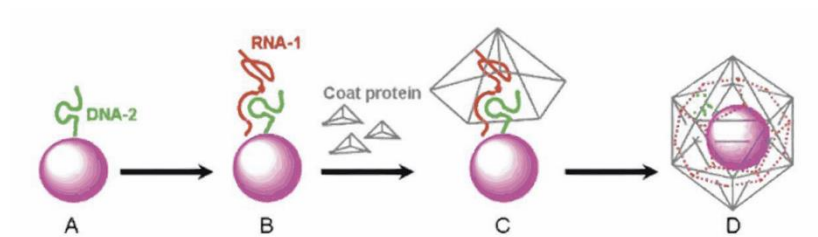


Figure 5.

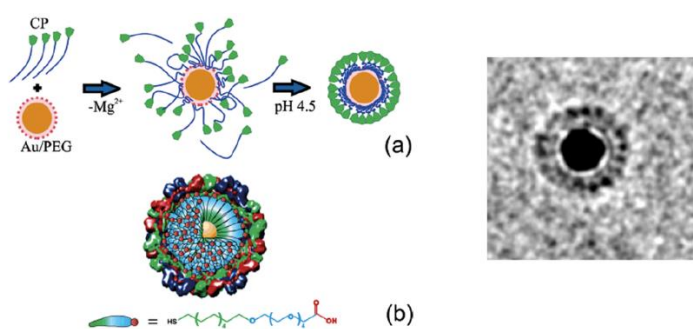


Figure 6.

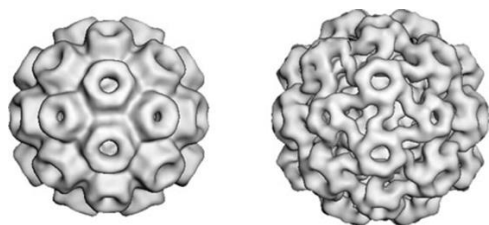


Figure 7.

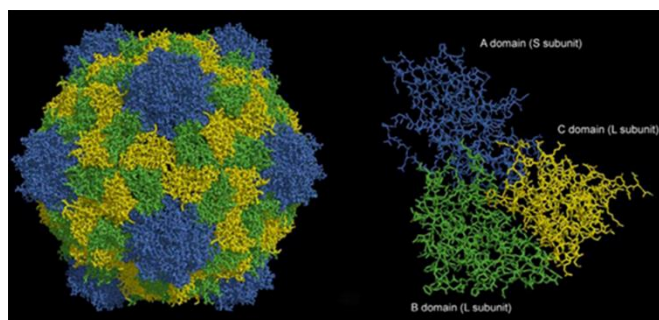


Figure 8.

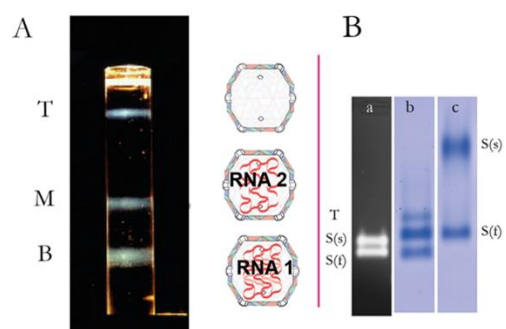


Figure 9.

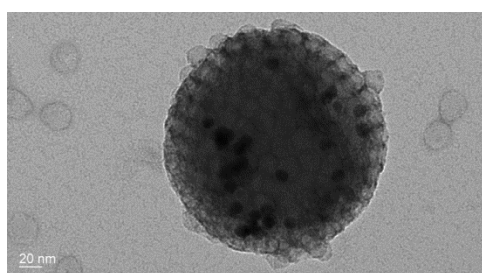


Figure 10.

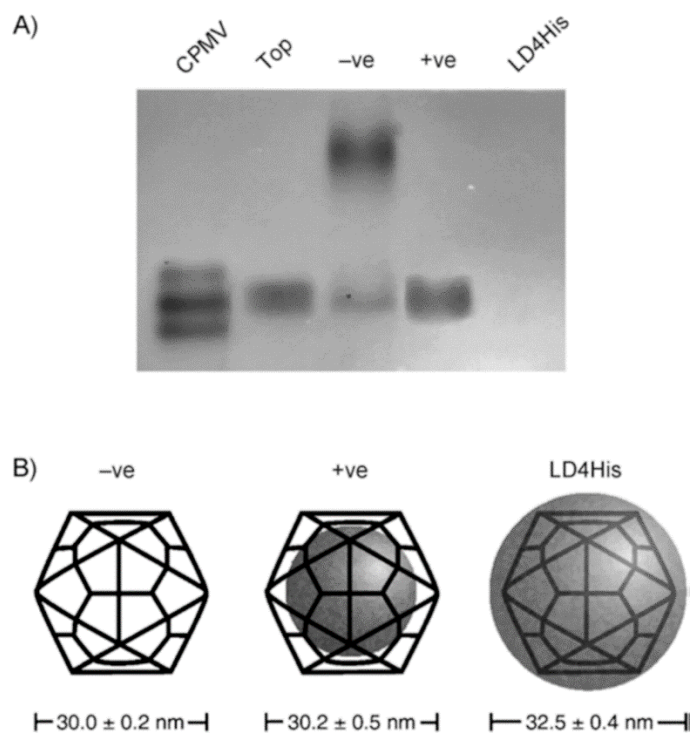


Figure 11.

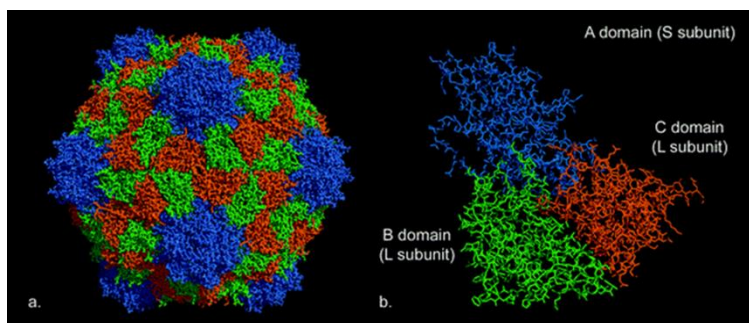


Figure 12.

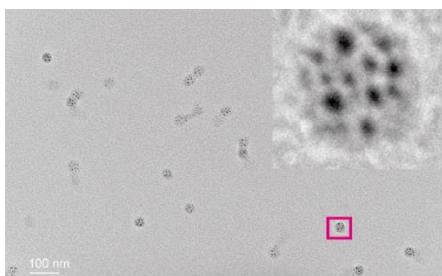


Figure 13.

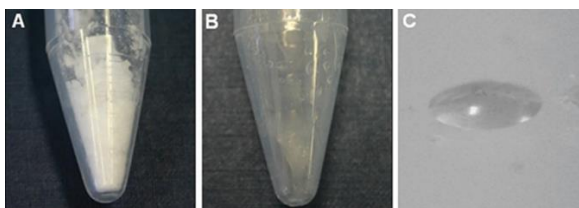


Figure 14.

